https://doi.org/10.5194/acp-2021-867
Preprint. Discussion started: 13 December 2021

Atmospheric Chemistry and Physics Discussions

Siberian Arctic black carbon: gas flaring and wildfire impact

Olga B. Popovicheva[1], Nikolaos Evangeliou[2,*], Vasilii O. Kobelev[3], Marina A. Chichaeva[4], Konstantinos Eleftheriadis[5], Asta Gregorič[6,7], Nikolay S. Kasimov[4]

[1] SINP, Lomonosov Moscow State University, 119991 Moscow, Russia
[2] NILU - Norwegian Institute for Air Research, 2007 Kjeller, Norway
[3]Moscow Department of Russian Geographical Society, Moscow, Russia
[4]Geographical Department, Lomonosov Moscow State University, 119991 Moscow, Russia
[5]ERL, Institute of Nuclear and Radiological Science & Technology, Energy & Safety, N.C.S.R. Demokritos, 15341 Attiki, Greece
[6]Aerosol d.o.o., SI-1000, Ljubljana, Slovenia
[7]Center for Atmospheric Research, University of Nova Gorica, SI-5270, Ajdovščina, Slovenia

* Corresponding authors: N. Evangeliou (Nikolaos.Evangeliou@nilu.no)

https://doi.org/10.5194/acp-2021-867
Preprint. Discussion started: 13 December 2021

Atmospheric Chemistry and Physics Discussions

Abstract

As explained in the latest Arctic Monitoring and Assessment Programme (AMAP) report released in early 2021, the Arctic has warmed three times more quickly than the planet as a whole, and faster than previously thought. The Siberian Arctic is of great interest largely because observations are sparse or largely lacking. A research aerosol station has been developed on the Bely Island, Kara Sea, in Western Siberia. Measurements of equivalent black carbon (EBC) concentrations were carried out at the "Island Bely" station continuously from August 2019 to November 2020. The source origin of the measured EBC, and the main contributing sources were assessed using atmospheric transport modelling coupled with the most updated emission inventories for anthropogenic and biomass burning sources of BC.

The obtained BC climatology for BC during the period of measurements showed a seasonal variation comprising the highest concentrations between December and April (60±92 ng/m3) and the lowest between June and September (18±72 ng/m3), typical of the Arctic Haze seasonality reported elsewhere. When air masses arrived at the station through the biggest oil and gas extraction regions of Kazakhstan, Volga-Ural, Komi, Nenets and Western Siberia, BC contribution from gas flaring dominated over domestic, industrial, and traffic sectors, ranging from 47 to 68%, with a maximum contribution in January. When air was transported from Europe during the cold season, emissions from transportation became important. Accordingly, shipping emissions increased due to the touristic cruise activities and the ice retreat in summertime. Biomass burning (BB) played the biggest role between April and October, contributing 81% at maximum in June. Long-range transport of BB aerosols appear to induce large variability to the Absorption Ångström Exponent (AAE) with values ranging from 1.2 to 1.4. As regards to the continental contribution to surface BC at the "Island Bely" station, Russian emissions dominated during the whole year, while European and Asian emissions contributed up to 20% in the cold period. Quantification of several pollution episodes showed an increasing trend in surface concentrations and frequency during the cold period as the station is directly in the Siberian gateway of the highest anthropogenic pollution to the Russian Arctic.

https://doi.org/10.5194/acp-2021-867
Preprint. Discussion started: 13 December 2021

Atmospheric Chemistry and Physics Discussions

1 Introduction

Global carbon pollution is annually produced by burning of fossil fuel and biomass. Combustion emissions are increasingly recognized as an important source of chemically active aerosols. Black carbon (BC) originates from the incomplete combustion of fossil fuels and biomass burning; it is a short-lived climate forcer and absorbs incoming solar radiation and, therefore, is of high significance for the Arctic climate (Wang et al., 2011). The combined total effects of BC and sulfates cause an Arctic surface warming of +0.29 K explaining approximately 20% of the observed Arctic warming since the early 1980s (Ren et al., 2020). BC resides in the lowest atmospheric layer, affects aerosol-cloud interactions (Yun et al., 2013) and has a cloud and sea-ice feedback when deposited (Flanner, 2013), thus accelerating melting (Quinn et al., 2008).

Long-range transport to the Arctic carries among other aerosol constituents many tracers of anthropogenic activities and wildfires (Chang et al., 2011). (Winiger et al., 2016) showed that BC in Arctic Scandinavia is predominantly linked to emissions in Europe. Over the whole Arctic region (north of 66°N), Russia contributes 62% to surface BC (Zhu et al., 2020). Industrial and residential sources are responsible for the highest measured BC concentrations at the Tiksi station (Siberian Arctic) (Popovicheva et al., 2019b). (Stathopoulos et al., 2021) have demonstrated that the long term impact of light absorbing carbon in the high Arctic is three times higher in the cold period of the year compared to the warm period. There, fossil sources mostly prevail during winter-spring season, while biomass burning sources dominate during low BC concentration periods in summer (Winiger et al., 2017). Although BC dominates light absorption by atmospheric aerosols, other carbonaceous aerosol species (brown carbon, BrC) represent an important fraction of light absorption in the UV and near-UV spectrum, thus having an important role in the assessment of radiative forcing in the Arctic climate. Spectral dependence of the light absorption is generally described by the absorption Ångström exponent (AAE) which is typically used to differentiate between different aerosol types (BC, BrC) and for the source apportionment of BC (Sandradewi et al., 2008; Helin et al., 2021; Zotter et al., 2017).

Quantification of the particulate Arctic pollution is a serious problem worldwide; reliable source emission inventories are challenged, and regional contributions of BC sources in the Arctic are still inconclusive (Zhu et al., 2020). Global anthropogenic emission dataset ECLIPSEv6 (Evaluating the Climate and Air Quality Impacts of Short-lived Pollutants) using the GAINS model (Klimont et al., 2017) includes all major economic sectors, such as energy and industrial production, transport, residential combustion, agriculture, and waste, distinguishing the sector-fuel-technology, fuels, and emission control options. The model predictions for European gateway

https://doi.org/10.5194/acp-2021-867
Preprint. Discussion started: 13 December 2021

to the Arctic were greatly improved when the emission inventory of anthropogenic sources was amended by estimates of European BC emissions (Winiger et al., 2016).

Due to large size and continuous production, gas flaring of oil industry is one of the highest BC emission sources (Ismail and Umukoro, 2012) with a strong environmental and climatic impact for the Arctic (Cho et al., 2019). Flaring in ECLIPSEv6 dominates BC emissions in the Arctic; models have found that flaring contributes 42% to the annual mean BC surface concentrations in the Arctic (Stohl et al., 2013). However, because flares are difficult to measure, their particulate emissions inventories and physicochemical properties are still underestimated (Conrad and Johnson, 2017; Popovicheva et al., 2019a). Currently, models are struggling to reproduce BC concentrations due to emission-related uncertainties in the Arctic region (Schacht et al., 2019). The observed annual mean contribution of fossil fuel combustion to the Arctic concentrations agrees within a factor of two (Qi and Wang, 2019).

The high latitude flaring emissions originate mainly from the North Sea, Norwegian Sea, the northeastern part of European Russia (Komi Republic) and Western Siberia. The largest oil and gas producing regions of northwestern Siberia are located along the main low-level pathway of air masses entering the Arctic and thus have a disproportionally large contribution to the Arctic lower troposphere (Stohl, 2006). (Eleftheriadis et al., 2009) and (Tunved et al., 2013) identified these regions as a key source for the highest measured BC concentrations and sub-micrometer aerosol mass concentration, respectively, at the Zeppelin station. The impact of BC long-range transport from northwestern Siberia was also observed at the Ice Base Cape Baranova station located on Severnaya Zemlya archipelago (Eastern Siberia) (Manousakas et al., 2020). Accordingly, possible gas flaring impact was observed at the Tiksi station (northeastern Siberia), despite the large distance of the station from the largest oil and gas producing regions (Winiger et al., 2017). To better understand and quantify the contribution of gas flaring to the Arctic environment, targeted aerosol and atmospheric composition measurements at the closest distance from the flaring facilities are needed. The present operating Eurasian Arctic stations are all too far away to allow assessing how air masses are affected by gas flares or what the contribution from different source categories is (Stohl et al., 2013). Simulations combined with observations of BC at the proximity of the source regions (e.g., the plumes from gas flaring regions over the Kara Sea) provide a better consistency (Popovicheva et al., 2017). In addition, measurements of BC coupled by conditional probability simulations performed at the Polar circle inside the oil and gas producing region of the northwestern Siberia have successfully separated the multiple industrial and urban sources (Popovicheva et al., 2020).

https://doi.org/10.5194/acp-2021-867
Preprint. Discussion started: 13 December 2021


Atmospheric Chemistry and Physics Discussions

Recent efforts have sought to develop a new Russian BC emission inventory (BCRUS) for the Siberian Arctic, based on activity data from local information, improved spatial distribution of BC emissions and updated emission factors for oil and gas fields in northwestern Siberia (Huang et al., 2015). It was found that BC emissions from gas flaring account for 36% of the total anthropogenic BC emissions over Russia. Residential BC emissions, transportation, industry, and power plants contribute 25%, 20%, 13%, and 5.4%, respectively. The emissions from the gas flaring sector in BCRUS show a discrepancy of more than 40% higher than ECLIPSEv5. Using BCRUS, modelled surface BC at stations Zeppelin, Barrow, and Alert were mostly improved (Huang et al., 2015). The contribution of anthropogenic emissions in Russia to the annual total Arctic surface BC were calculated to represent 56%, with gas flaring from the Yamalo-Nenets Autonomous Okrug (YNAO), Khanty-Mansiysk Autonomous Okrug (KMAO), and Komi Republic being the main source (31% of Arctic surface BC) (Zhu et al., 2020). However, due to the absence of an official BC inventory of industrial emissions and a denser observation network in the western Siberian high Arctic, the spatial distribution of BC sources is still associated with large uncertainties.

Agriculture fires in East Europe and North America are a major source of biomass burning in the Eurasian Arctic (Treffeisen et al., 2007; Stohl et al., 2007; Stohl et al., 2006). Springtime fires in Siberia can double the Northern American Arctic background (Warneke et al., 2010). Long-term airborne observations of BC in Northern Siberia have revealed a strong impact of forest fires in summer (Kozlov et al., 2016; Paris et al., 2009). Particulate brown carbon (BrC) has been reported to be emitted by intense wildfires and measured in plumes transported over two days (Forrister et al., 2015). In summer 2019, wildfire activity in Central and Eastern Siberia occurred during the trans-Arctic transport pathway of Siberian biomass burning emissions resulting in enhanced aerosol lamina observed in western Canada (Johnson et al., 2021).

In 2019, a new aerosol station was established by Moscow State University on the Bely Island located in the Kara (Western Siberian Arctic) (https://peexhq.home.blog/2019/12/11/new-research-aerosol-stations-in-the-russian-arctic), (Figure 1). The region was chosen because it is close to the air pathway of large-scale emission plumes from populated industrial regions of Eurasia and Siberian wildfires to the Arctic. We present here the ground-based continuous BC (equivalent BC, EBC) measurements from August 2019 until November 2020 at the "Island Bely" station for the first time. The Arctic annual trends of BC are assessed, while the geospatial source origin of the air arriving at the station is identified using a Lagrangian particle dispersion model. Furthermore, the anthropogenic and biomass burning contributions in the modelled surface concentrations of BC are evaluated against measured BC concentrations at Bely. Characterization

https://doi.org/10.5194/acp-2021-867
Preprint. Discussion started: 13 December 2021

Atmospheric Chemistry and Physics Discussions

of the pollution events in cold and warm periods distinguishes the higher impact of gas flaring versus biomass burning. The spectrally resolved absorption measurements provide an opportunity for the characterization of BC sources. The present study attempts to assess the extent of long range transported plumes from the large-scale emissions from the Eurasian continent is attributed to BC emitted in the Western Siberian Arctic, by means of modelling coupled with continuous observations.

2 Experimental

2.1 Aerosol station "Island Bely".

Western Siberia is the world's largest gas flaring region with a leading oil and gas production industry (**Figure *1***). YNAO is located north of the West Siberian Plain and covers a vast area of 769 thousand km^2. More than 94% of the region's economy is associated with industrial applications related to the extraction of fuels, their processing, and transportation. Specifically, YNAO has the largest reserves of Russia's natural gas and oil; YNAO's BC emissions approach a maximum through the Russian territory (Vinogradova, 2015). The relative contributions from gas flaring to annual mean BC surface concentrations from all emission sources (surface transportation, industry, residential, biomass burning) exceed 70% (Stohl et al., 2013).

The Bely Island is located in the Kara Sea, north of the YNAO (**Figure *1***). For the purpose of atmospheric composition observations and sampling at the "Island Bely" station, the aerosol pavilion has been built approximately half a km to the southeast of the Roshydromet meteorological station continuously operating at the island (**Figure *1***). There are no other anthropogenic constructions on the island. Thus, the major advantage of a new-developed research station is its long distance from any local anthropogenic sources. Previous research at the Tiksi station has shown significant aerosol pollution from local sources (Popovicheva et al., 2019), which is not the case in the "Island Bely" station.

An Aethalometer model AE33 (Magee Scientific,Aerosol d.o.o.) was used to measure the light attenuation caused by particles depositing on two filter spots at different flow rates (Drinovec et al., 2015) at seven wavelengths from ultraviolet (370 nm) to infrared (950 nm). The "dual spot" technique is applied for real-time loading effect compensation. The light-absorbing content of carbonaceous aerosol at 880 nm is reported as equivalent black carbon concentration (EBC), which is determined for each time interval from the change in the light attenuation at a wavelength of 880, using a mass absorption cross-section of 7.7 m2/g and filter multiple scattering parameter C of 1.57. Light absorbing organic components (BrC) absorb light at shorter wavelengths more effectively than at 880 nm, which is observed as an increased AAE (Sandradewi et al., 2008;

https://doi.org/10.5194/acp-2021-867
Preprint. Discussion started: 13 December 2021


Atmospheric Chemistry and Physics Discussions

Grange et al., 2020; Helin et al., 2021). AAE was calculated using Eq. 1 for 470 nm and 950 nm wavelengths:

$$AAE = \frac{\ln(babs(470)/babs(950))}{\ln(950/470)} \quad (1)$$

where b_{abs} stands for the absorption coefficient at 470 nm and 950 nm. In order to avoid instrumental noise when calculating the AAE, the following data processing was implemented. One-minute absorption coefficients for the whole period were averaged to 1 hour. The dataset was filtered to periods when EBC exceeded 20 ng/m^3 (sensitivity level at 1 hour time resolution), then the AAE was calculated from 3-hour averaged dataset.

The Aethalometer model (Sandradewi et al., 2008) is typically used for the source apportionment of EBC, when measurements of absorption coefficient are performed by filter photometers. The model uses an apriori assumed pair of AAE for traffic (AAETR) and biomass burning (AAEBB) to determine the contribution of both sources. Although the Aethalometer model is an efficient tool for source apportionment of EBC in a well-mixed urban atmosphere, where two sources with distinct aerosol optical properties prevail (fossil fuel from traffic and fresh biomass burning), the model results can be affected when the characteristic optical properties of a specific source change over time. This is usually true with wildfires, where different burning modes (flaming or smoldering) and different type of wood can significantly influence the BrC emission and its chemical composition (Kalogridis et al., 2018b). Furthermore, chemical evolution after the emissions and atmospheric aging (i.e. aerosol mixing state, particle morphology and size distribution) additionally influence aerosol absorption, which can be noticed especially for the long-range transported air masses (Cappa et al., 2016; Saleh et al., 2013; Romshoo et al., 2021). (Forrister et al., 2015) have shown that BrC emitted from wildfires was highly unstable, with 6% of BrC remaining above background levels after two days. However, the remaining increase over the background can importantly influence the radiative forcing in the Arctic environment.

BC measurements at the “Island Bely” station were performed from 10 August 2019 to 30 November 2020, with a time resolution of 1 min. For screening the BC data, we used the measured wind direction. In that case, strong BC spikes that coincided with wind directions related to local diesel sources were removed from further data analyses. The basic meteorological parameters, such as temperature, wind speed and direction were obtained every 3 hours by a meteorological station located 500 m from the “Island Bely” station.

2.2 Atmospheric transport model coupling with emissions

https://doi.org/10.5194/acp-2021-867
Preprint. Discussion started: 13 December 2021

Atmospheric Chemistry and Physics Discussions

To investigate the possible origin of BC, the Lagrangian particle dispersion model FLEXPART (FLEXible PARTicle dispersion model) version 10.4 was used (Pisso et al., 2019). The model was driven by 3-hourly operational meteorological fields from the European Centre for Medium-Range Weather Forecasts (ECMWF) with 137 vertical levels and a horizontal resolution of 1°×1°. In FLEXPART, computational particles were released at height 100 m from the receptor ("Island Bely" station) and were tracked backward in time in FLEXPART's "retroplume" mode. Simulations extended over 30 days backward in time, sufficient to include most BC emissions arriving at the station, given a typical lifetime of 1 week (Bond et al., 2013).

The tracking includes gravitational settling for spherical particles of the size observed. FLEXPART differs from trajectory models due to its ability to simulate dry and wet deposition of gases or aerosols (Grythe et al., 2017), turbulence (Cassiani et al., 2015), unresolved mesoscale motions (Stohl et al., 2005), while it includes a deep convection scheme (Forster et al., 2007). For our simulations, we assumed that BC has a density of 1500 kg m^{-3} and follows a logarithmic size distribution with an aerodynamic mean diameter of 0.25 μm and a logarithmic standard deviation of 0.3 (Long et al., 2013) .

FLEXPART simulations were performed every 3 hours during the studied period. The FLEXPART output consists of an emission sensitivity which yields a simulated concentration in the receptor box when coupled with gridded emissions from an inventory. The emission sensitivity can also be interpreted as a probability distribution field of the particle origin. The source contributions to Arctic BC were derived by incorporating the gridded retention time into the column emission flux, which was adopted from the emission inventories in each grid-cell. Calculations for anthropogenic sources (different emission sectors are described below) and open biomass burning were performed separately. This enabled identification of the exact origin of BC and allowed for quantification of its source contribution. The source contribution can also be displayed as a function of the time elapsed since the emission has occurred (i.e., "age"), which can be shown as "age spectrum".

In this study, anthropogenic emission fluxes were adopted from the lastest version (v6b) of the ECLIPSE (Evaluating the CLimate and Air Quality ImPacts of ShortlivEd Pollutants) dataset, an upgraded version of the previous version (Klimont et al., 2017). The inventory includes industrial combustion (IND) emissions from industrial boilers and industrial production processes. Energy production sector (ENE) includes emissions from combustion processes in power plants and generators. Residential and commercial sector (DOM) includes emissions from combustion in heating and cooking stoves and boilers in households and public and commercial buildings. Waste treatment and disposal sector (WST) resembles emissions from waste incineration and treatment.

https://doi.org/10.5194/acp-2021-867
Preprint. Discussion started: 13 December 2021


Atmospheric Chemistry and Physics Discussions

Transport sector (TRA) includes emissions from all land-based transport of goods, animals and persons on road networks and off-road activities. Emissions from shipping activities in in-land waters (SHP) is included as a separate sector. Gas flaring (FLR) sector includes emissions from oil and gas facilities. The methodology for obtaining emissions from FLR specifically over Russia has been improved in ECLIPSEv6 (Böttcher et al., 2021). Updates were based on new field-type specific emission factors that were applied to VIIRS observations of the flared gas volume at individual flaring locations. For comparison, BCRUS emissions for the FLR sector (Huang et al., 2015) were also used in this study.

Emissions from biomass burning (BB) were adopted from Copernicus Atmosphere Monitoring Services (CAMS) Global Fire Assimilation System (GFAS). CAMS GFAS assimilates fire radiative power (FRP) observations from satellite-based sensors converting the energy released during fire combustion into gases and aerosol daily fluxes (Di Giuseppe et al., 2016; Kaiser et al., 2012). Data are available globally on a regular grid with a horizontal resolution of 0.1 degrees from 2003 to the present. FRP observations assimilated in GFAS are the NASA Terra MODIS and Aqua MODIS active fire products (http://modis-fire.umd.edu/, (Kaufman et al., 2003). FRP measures the heat power emitted by fires, as a result of the combustion process and is directly related to the total biomass combusted (Wooster et al., 2005). Using land-use-dependent conversion factors, GFAS converts FRP into emission estimates of 44 smoke constituents (Kaiser et al., 2012). We used BC emissions in this study.

Biomass burning emissions were also adopted from the Global Fire Emission Dataset version 4.1 (GFEDv4.1). The product combines satellite information on fire activity and vegetation productivity to estimate gridded monthly burned area and fire emissions, as well as scalars that can be used to calculate higher temporal resolution emissions. All data are publicly available for use in large-scale atmospheric and biogeochemical studies and include (i) burned area (Giglio et al., 2013) , (ii) burned area from "small" fires based on active fire detections outside the burned area maps detailed in (Randerson et al., 2012) and updates in (Werf et al., 2017), (iii) carbon and dry matter emissions from van der Werf et al. (2017), (iv) fractional contributions of various fire types to total emissions and (v) list of emission factors to compute trace gas and aerosol emissions based on (Akagi et al., 2011) and (Andreae and Merlet, 2001). The current version (v4) has a spatial resolution of 0.25 degrees and is available from 1997 onwards.

In the present paper, several different configurations were used to calculated modelled surface BC concentrations at “Island Bely” station, namely ECLIPSEv6 with GFED4 (ECLIPSEv6-GFED4), and ECLIPSEv6 with CAMS (ECLIPSEv6-CAMS). The same two

https://doi.org/10.5194/acp-2021-867
Preprint. Discussion started: 13 December 2021


Atmospheric Chemistry and Physics Discussions

277 configurations were also used after substituting the FLR emissions in ECLIPSEv6 with those from
278 BCRUS (Huang et al., 2015).

279 3 Results and discussion

280 3.1 Monthly climatology of black carbon

281 The climate at the Bely Island is characterized by an average annual temperature of -8°C,
282 precipitation of 450 mm, and stable snow coverage from October to May. Meteorology displays a
283 large annual variability determined by alternating periods of the polar night and midnight sun.
284 Median temperatures stay above 0°C for 4 months each year between June and September. This
285 period is also characterized by the highest-frequency occurrence of ocean air masses and the most
286 stable wind speeds. A shift occurred in October with decreased solar insolation resulting in a
287 temperature shift to below 0°C. The cold month winds were primarily continental, with a low-
288 frequency occurrence of ocean air masses.

289 The cycle of the temperature and wind speed variation observed during the study period is
290 shown in **Figure *2***a,b. Period from 1 November 2019 to 1 April 2020 when temperature dropped
291 below -10 ^{0}C, as well as November 2020, is denoted as the "cold period" in the present paper. The
292 remaining period of our study, from 10 August to 31 October 2019 as well as from April to 1
293 November 2020, is considered as the "warm period". **Figure *2***c illustrates the long-term time
294 series of 24h median EBC concentrations measured at wavelength of 880 nm (EBC(880)) during
295 the study period, with median value 37±64 ng/m^3, maximum and minimum of 520 and 6 ng/m^3,
296 respectively.The polar frequency plot of wind speed/directions shows that the maximum number
297 of hours the wind was from north-east and south-west directions with around 5 m/s (**Figure 3**a).
298 BC concentration roses in **Figure 3** indicate the sources of highest concentrations, which
299 originated from the continent in both cold and warm periods.

300 **Figure 4** illustrates a long-term time series of monthly EBC concentrations at the "Island
301 Bely" station during the period from August 2019 to November 2020. The highest EBC
302 concentrations were observed from November to April and the lowest ones from June to August,
303 in agreement with the typical seasonal trend of the Arctic aerosol concentrations (Stone et al.,
304 2014). EBC monthly climatology during the study period is shown in **Figure *4***a in terms of the
305 median, and upper and lower quartiles. For winter months, the maximum median EBC
306 concentration was 165 ng/m^3 in December 2019. The increase of the Arctic concentrations in
307 winter, known as the Arctic Haze, was more pronounced in November-December 2019 and
308 January-March 2020. On average, concentrations in summer were about 10 times lower than those
309 in winter, with a minimum median value of 30 ng/m^3 in July 2020.

https://doi.org/10.5194/acp-2021-867
Preprint. Discussion started: 13 December 2021

Atmospheric Chemistry and Physics Discussions

Observations at the "Island Bely" station of the second year started from August 2020 and lasted to November 2020 to confirm the general annual trend of low summer and high winter BC concentrations. However, monthly median EBC in September 2020 demonstrated the unprecedented high value of 72 ng/m^3, twice as much as in September 2019.

Similar annual trend was recorded in 2015-2016 at the Tiksi station (coast of Laptev sea), with high concentrations reaching 130 ng/m^3 during winter-spring and low concentrations of about 20 ng/m^3 observed from May to October (Popovicheva et al., 2019b). As shown by earlier studies at various polar stations, such as in Ny-Ålesund, Alert, and Barrow, aerosols display Arctic Haze peak concentrations during winter and early spring months (Stone et al., 2014). EBC during Arctic Haze at both "Island Bely" and Tiksi stations are found higher in comparison to observed ones at Alert (100±65 ng/m^3), which has shown maximum concentrations among all Polar stations (Sharma et al., 2004). The latter confirms previous findings from (Eckhardt et al., 2015) and (Winiger et al., 2017) that the Siberian Arctic is mainly polluted due to the influence of emissions from the Eurasian continent.

Near-surface measurements allow for evaluation of the capability of a transport model to reproduce the distribution of BC in the Arctic based on different emission datasets (Schacht et al., 2019; Zhu et al., 2020). **Figure *4***a and Supplentary Table S 1 show observed and modelled BC monthly median mass concentrations at the "Island Bely" station. Use of ECLIPSEv6 emissions cause overestimations of modelled BC concentrations of up to 46% (February 2020). All simulated BC concentrations were found in the range between the 25th and 75th percentiles of measured EBC. Modelled BC is underestimated in March-May 2020, being 29 ng/m^3 below the 25th percentile of EBC in April 2020. When the FLR emissions in ECLIPSEv6 were substituted by BCRUS flaring, similar modelled BC monthly median concentrations were calculated, thus indicating that other sectorial emissions might have large contribution to surface BC at the "Island Bely" station.

FLEXPART simulations that extended over 30 days back in time can be displayed as a function of the time elapsed since the emission has occurred (age spectrum). **Figure *4***b shows the contribution of a certain age (days backwards) estimated for the "Island Bely" station. In the cold period of high EBC concentrations, the longest age of more than 19 days back, affects up to 60% of the surface BC. In this time, due to the geographical proximity, Russia dominates; however, both Europe and Asia contribute around 20% to the monthly averaged surface BC, with the biggest contribution to be in February 2019 and November 2020, (**Figure *4***b,d). The most aged air masses (from 28 to 30 days back) contributed up to 50%, arriving at the "Island Bely" station in December 2019, which is the month of the highest observed EBC concentrations during the study period. The

https://doi.org/10.5194/acp-2021-867
Preprint. Discussion started: 13 December 2021


Atmospheric Chemistry and Physics Discussions

343 impact of the closest regions with age between 7 and 9 days is the most significant in winter
344 months, while in the warm period, such short-term contributions become negligible.

345 The calculated age and continental spectrum of BC obtained for the "Island Bely" station
346 mainly denote the variability of airmass transport patterns in different seasons. In the cold season,
347 the Siberian Arctic tends to force the air from south to north into the Arctic (Stohl, 2006), thus
348 bringing more anthropogenic BC northward from highly populated regions.

349 Monthly averaged BC contributions from different sources simulated by FLEXPART with
350 ECLIPSEv6 emissions are shown in **Figure *4*c** and Supplementary Table S 2. From November
351 2019 to March 2020 the FLR sector contributed 47%–68% (maximum in January 2020) to surface
352 BC, when air masses arrived at the Bely Island through oil and gas extraction sites. February and
353 November 2020 demonstrated the biggest non-gas flaring impact, indicating that air masses passed
354 through highly populated regions. Especially February 2020 coincides with the largest model
355 overestimation, (**Figure 4**a), implying likely misestimation of non-gas flaring emissions in
356 ECLIPSEv6. From April 2020 the impact of FLR dropped significantly (Supplementary Table S
357 3), with minimum of 12% in June. Starting from April to October 2020, BB emissions played the
358 biggest role in surface BC contribution, approaching 81% in June 2020. It is noteworthy that the
359 impact of SHP emissions became quite distinguished in a warm period when the ocean ice cover
360 is absent in the Arctic and touristic cruises peak.

361 Emission sensitivities of surface BC presented over the whole Arctic (north of 66°N) have
362 been also simulated using the same model as in the present in (Zhu et al., 2020). Anthropogenic
363 sources contributed 82% of the annual BC, as estimated from BCRUS emission dataset. Arctic BC
364 originated predominantly from anthropogenic emissions in Russia (56%), with FLR from YNAO,
365 Khanty-Mansiysk Autonomous Okrug (KMAO), and Komi Republic being the main source (31%
366 of Arctic surface BC). In summer (July-August), open BB in Siberia, Alaska, and Canada
367 contributed 75%. At Zeppelin, modelled BC (39.1 ng/m^3 for annual mean) was reported to be 85%
368 higher than the observed value (21.1 ng/m^3 for annual mean)(Zhu et al., 2020). At the Tiksi station,
369 modelled BC was underestimated (74.4 ng/m^3 for annual mean) by 40% in comparison with the
370 observations (104.2 ng/m^3 for annual mean) (Zhu et al., 2020). Annual (from September 2019 to
371 August 2020) median modelled concentrations of BC using ECLIPSEv6, BCRUS, and CAMS for
372 the "Island Bely" station are shown in Supplementary Table S 1. We find that modelled BC (78.4
373 ng/m^3 for annual mean) is 26% higher than the observed value (61.8 ng/m^3 for annual mean); the
374 overestimation is much smaller than observed for other remote stations. Annual averaged
375 contributions of anthropogenic emissions by ECLIPSEv6 and ECLIPSEv6 with flaring from

https://doi.org/10.5194/acp-2021-867
Preprint. Discussion started: 13 December 2021


Atmospheric Chemistry and Physics Discussions

BCRUS were equal to 76% and 80%, respectively, in conjunction with the respective contribution of the FLR sector from the two dataset (Supplemental Table S 3).

3.2 Cold season pollution

Figure *5*a shows EBC concentrations measured at the "Island Bely" station during the cold period, from November 2019 to April 2020 as well as from 1st to 30th November 2020. Time series indicates that EBC undergoes the characteristic Arctic seasonal trend with higher concentrations in winter and early spring and lower in summer. Background pollutant concentrations in the Arctic stations are generally very low without any detectable influence of local or regional pollution (Eleftheriadis et al., 2004; Popovicheva et al., 2019b). We relate the Arctic background to the lowest 20th percentile of EBC data (10 ng/m^3). Long-term pollution episodes were assumed to be repeated events of high EBC concentration above the 80th percentiles (90 ng/m^3) that are clearly distinguishable from the background, (**Figure *5***a).

The aerosol optical properties with respect to absorption, presented as daily median AAE are shown in **Figure *2***d. The AAE for the highly aged aerosols measured during the periods of low BC was lower than 1, reaching values as low as 0.2, which is addressed mostly to the aerosol size distribution (large particles) and internally mixed BC particles (Cappa et al., 2016). As shown by modeling studies (Virkkula, 2021), pure BC particles coated by non-absorbing coating can have AAE in the range from <1 to 1.7, depending also on the morphology of the fractal aggregates (Romshoo et al., 2021). The AAE becomes more reliable in periods of higher aerosol concentration levels in the cold period, when it ranged from 0.6 to 1.35.

When AAE exceeded 1 in the cold period, the pollution periods can be identified as influenced by BB. Due to the mixing with background aerosol and ageing processes, the air mass influenced by BB events is expected to have increased AAE as compared to BC produced by fossil fuel. However, ageing processes may induce a high variability in AAE observed values at receptor areas of long range transported pollution and AAE may not be representative of BB sources. Nevertheless, it can still be used as a qualitative parameter, when extra information is available. Such events of increased AAE were rarely observed in our study, and the most prominent BB impact occurred during the pollution episode P4, P7, and P8 when impact of domestic sources was the most prominent (**Figure *5***a).

Generally, FLEXPART with ECLIPSEv6-CAMS emissions captures periods with both high and low concentrations relatively well, (**Figure *2***c). A good correlation between measurements and simulations, with a Pearson coefficient R of 0.7 and the root mean squared error **(**RMSE) of 89.2 ng/m^3, is obtained for the cold period (**Figure *6***a). According to monthly median

https://doi.org/10.5194/acp-2021-867
Preprint. Discussion started: 13 December 2021


Atmospheric Chemistry and Physics Discussions

409 contributions to BC concentrations in the cold period, the impact of anthropogenic sources, namely
410 FLR, DOM and TRA dominated surface BC by 97.7% (**Figure *5***b).

411 Looking closely to specific episodes, during pollution P1, three events of high EBC
412 concentrations were observed, (**Figure *5***a). On 5 November 2019, measured EBC reached 180
413 ng/m^3, while FLEXPART simulated similarly high BC values. Footprint emission sensitivities at
414 this time showed that airmasses originated from East and North Europe, passed south of European
415 Russia, then turned the direction straight through the West Siberia approaching the Bely Island
416 from the southeast (**Figure *7***). This airmass moved towards the large Russian FLR sources of
417 YNAO, KMAO, and Krasnoyarsky Krai (see **Figure *1***) causing up to 71% contribution to surface
418 BC (Supplementary Table S 4).

419 On 12 November 2019, airmasses arrived at the Bely Island through the Yamal peninsula
420 after passing the ocean (Supplementary Figure S 1). Model strongly underestimated measured
421 EBC concentrations by about 10 times (**Figure *7***). We fail to provide a concrete explanation for
422 this; a simplified hypothesis is that a number of fields located at the Yamal peninsula might have
423 not been inluded into the emission database, but this certainly needs further research. In contrast,
424 the model strongly overestimated measured EBC concentrations on 16 November 2019. At that
425 time, airmasses passed through remote regions of Eastern Siberia and arrived through the gas
426 flaring sites of Krasnoyarsky Krai at the station (**Figure *7***) causing an FLR contribution of 98.6%
427 to surface BC (Supplementary Table S 4). The reason might be use of incorrect emission factors
428 for BC at the FLR facilities of Krasnoyarsky Krai in the adopted emissions, because direct
429 transport from this region was observed. During 12 and 16 November 2019 the AAE was in the
430 range from 0.7 to 1, which agrees with the expected optical properties for the FLR sources.

431 Pollution episode P2 in December 2019 gave the highest EBC concentrations observed
432 during the whole cold period, (**Figure *5***a). On 4 December, EBC approched 400 ng/m^3, when
433 airmasses originated from Kazakhstan and Russian gas flaring regions of KMAO and YNAO
434 (**Figure *8***) reached the Bely Island. The maximum EBC concentration of approximately 500 ng/m^3
435 with AAE 1.05 was observed on 19 December, when air was came from Europe, initially through
436 the Russian oil and gas basins of Volga-Ural at the south of European Russia and then through
437 KMAO and YNAO in Western Siberia (**Figure *8***). During the December pollution events, FLR
438 contribution dominated, reaching 73% on 19 December (Supplementary Table S 4).

439 The highest FLR contributions were observed during the pollution episodes P3-P6
440 (Supplementary Table S 4). Similar airmass transportation through either gas and oil fields of

https://doi.org/10.5194/acp-2021-867
Preprint. Discussion started: 13 December 2021


Atmospheric Chemistry and Physics Discussions

YNAO and KMAO in Western Siberia or Komi and Nenets regions north of European Russia occurred for all events, (Supplementary Figure S 1).

In contrast to the aforementioned events, the pollution episode P7 was unrelated to FLR, as airmasses did not cross the flaring regions (**Figure *8***). On 16 November 2020, retroplumes confirm origin of the surface BC from Central and Eastern Europe and the Kola Peninsula (**Figure *8***). DOM and TRA hold the largest share of the source contribution with 73% and 20%, respectively (Supplementary Table S 4), while the model overestimated measured EBC. Episode P8 gave the biggest EBC (370) concentration which reached 346 ng/m^3 and exceeded EBC(880) (133 ng/m^3) on 24 November 2020 (Supplementary Table S 4). At that time, airmasses came to the Bely Island directly from the most populated region of European part of Russia (**Figure *8***). The contribution of DOM and TRA was 34% and 23%, respectively. AAE approached the highest value observed (1.3) during the study period. Thus, it addresses a detectable impact of biomass burning in the classified DOM emissions. BC from wood burning contributes around 61% of the total residential emissions, especially in areas where there is limited use of natural gas (Kalogridis et al., 2018a), and in forest regions (Huang et al., 2015). Note that the impact of IND emissions was the largest in P7 and P8 events as compared to the whole cold period (Supplementary Table S 4), due to industrial emissions from sites in Central European Russia.

3.3 Warm season pollution

Figure *5*b shows EBC concentrations measured at the "Island Bely" station during the warm period, from 10 August to 31 October 2019 and from 1 April to 1 November 2020. It is immediately seen that BC in the warm period was mainly affected by Russian emissions (90%), and only in October 2020 and August 2019 partly (~20%) from Europe and North America, (**Figure *4***). EBC concentrations rarely exceeded the 80th percentile that was set as the pollution criterion, while the duration of the warm period episodes was shorter.

Due to the mixing with background aerosol and ageing processes, the air masses influenced by BB events is expected to have increased AAE as compared to the BC produced by fossil fuel. However, ageing processes may induce a high variability in AAE at receptor areas of long-range transported pollution and the AAE may not be representative of a BB aerosol source. It is used here as a qualitative tool. Pollution events were rarely observed in this season, and the most prominent BB impact occurred during the pollution episodes P4, P7, and P8.

However, the events characterised by higher AAE were observed more frequently, indicating that the impact of BB was more significant during the warm period, mainly during spring and summer (episodes P3,P4, and P6). Comparison between measured and modelled

https://doi.org/10.5194/acp-2021-867
Preprint. Discussion started: 13 December 2021


Atmospheric Chemistry and Physics Discussions

concentrations showed poor correlation (R of 0.41 and RMSE of 121 ng/m^3) (**Figure *6***). According to monthly median contributions to BC concentrations in the warm period, the impact of BB emissions was as high as 50% (**Figure *4***c). SHP emissions contributed about 1%, as a result of the increase of touristic activity in the Arctic and the more active use of the Northern Sea Route due to the Arctic ice retreat.

From the beginning of the study period in August 2019, large wildfires were observed in Siberia (Voronova et al., 2020). The latter resulted in a strong BB impact into the Arctic BC at the "Island Bely" station (**Figure *5***c). However, during event P1, the observed EBC concentrations of approximately 200 ng/m^3 were not caused by the wildfire plumes (**Figure *5***). During this time, airmasses were transported from Northern Europe (Supplementary Figure S 1), and the main contribution to the surface BC at the "Island Bely" station was due to TRA emissions (36%, Supplementary Table S 4).

Episode P2 during October 2019 (**Figure *5***) was characterised by high EBC of 119 ng/m^3. Modelled concentrations were strongly overestimated (Supplementary Figure S 1). The calculated BB contribution to the surface BC was 64% (Supplementary Table S 4) and the hotspot BB sources were near the Pur River (YNAO) as recorded by CAMS (Supplementary Figure S 1). The measured AAE does not indicate any contribution of BrC, which would be expected for BB sources. AAE values observed during the P2 episode were lower than 1 (Supplementary Table S 4). Note that the FIRMS active fire data analyses (https://firms.modaps.eosdis.nasa.gov/) indicate that the fire spots were in the same grid-cell as industrial facilities of oil extraction field in the Purovski region (YNAO). Thus, it might be that thermal anomalies from flaring facilities were mistakenly related to fires in CAMS. This hypothesis is reinforced by the fact that no wildfires were recorded by the local forest fire service (https://aviales.ru) during October 2020 in Western Siberia and Krasnoyarsky Krai.

Pollution episode P3 is related to strong springtime wildfire activity that occurred in Southern Siberia. The retroplumes on 18 and 23 April 2020 showed that the air originated from Central Asia, a large territory of Southern Siberia and Krasnoyarsk Kray arriving at the Bely Island through the Western Siberia from the southeast (Supplementary Figure S 1, **Figure *9***). High footprint emission sensitivities coincided with the location of large wildfires resulting in BB contribution to surface BC at the "Island Bely" station equal to 28% and 19%, respectively. The most significant impact of wildfires was observed on 23 April 2020, when 6-hour median EBC concentration reached 700 ng/m3 with AAE ranging from 1.3 to 1.5, clearly indicating an elevated contribution of BrC (Supplementary Table S 4).

https://doi.org/10.5194/acp-2021-867
Preprint. Discussion started: 13 December 2021


Atmospheric Chemistry and Physics Discussions

Wildfires occurred in northern Krasnoyarsk Krai and Sakha Republic, Central Siberia between April and November 2020 (https://aviales.ru/popup.aspx?news=6286) burning around seven million hectares of forest. The pollution episode P4 was recorded at the "Island Bely" station on 7 July 2020, with 6-h median EBC of 150 ng/m^3 and AAE around 1.4 indicating BB impact. The model captures this event well, providing the highest BB contribution exactly when observed, equal to 90%, (Supplementary Table S 4). Airmasses arrived from the east and passed north of Krasnoyarsk Kray (**Figure *9***).

Unprecedented high wildfire-related BC concentration was observed in September 2020 (pollution episode P6). EBC concentrations exceeded 5 and 20 times the 80th percentile of the measurements. Maximum 6-h median EBC reached 534 ng/m^3 on 1st September 2020 that was even higher than the biggest Arctic haze concentration observed in December 2019, (Supplementary Table S 4). Increased AAE of around 1.4 indicted prominent BB impact. Such a strong event resulted from long-range transport of BC from the Eurasian continent during the intensive wildfires in Western Siberia (Krasnoyarsk Kray and Yakutia) (**Figure *9***); there, around one million hectares of forest were burned in August 2020. The contribution of BB to surface BC at "Island Bely" was as high as 95%.

Despite the exclusive BB origin of the light absorbing carbon measured at the "Island Bely" station, the AAE is much lower than the established value for fresh BB (close to 2) (Sandradewi et al., 2008) likely due to ageing. This apparent reduction of the BrC contribution to absorption is in agreement with (Forrister et al., 2015) which examined BrC concentrations and AAE of Western U.S. forest fires as a function of aging. Their result shows that most BrC (~94%) emitted from wildfires was lost within a day. Similar observations have been reported for long-range transported North American smoke over the Northeastern Atlantic (Zheng et al., 2020) and long range transported Russian smoke over the Mediterranean (Diapouli et al., 2014).

The last pollution episode P7 was observed at the end of October 2020. Although it occurred in the warm period, it is rather related to Russian FLR and European TRA emissions (Supplementary Table S 4, **Figure *5***b). At the end of October 2020 air came mainly from Europe, passing through the Yamal Peninsula.

4 Conclusions

The present paper aims at performing a quantitative analysis of the Arctic pollution via high-resolution measurements from a recently developed aerosol station at the Bely Island (Kara Sea) combined with Lagrangian modelling. A consequent goal is to examine the impact of anthropogenic and natural sources to the high Arctic as a result long-range transport. The main results can be summarised as follows:

https://doi.org/10.5194/acp-2021-867
Preprint. Discussion started: 13 December 2021


Atmospheric Chemistry and Physics Discussions

- EBC monthly climatology is following the typical Arctic aerosol seasonal variation characterised with higher EBC concentrations in winter and lower in summer.
- AAE for aged BC between 1 and 1.35 indicates wood burning impact from domestic activity and/or wildfires in both periods examined.
- The recently upgraded ECLIPSEv6 emissions and ECLIPSEv6 coupled with flaring from BCRUS represent measured EBC accurately in the cold period. Annual average contributions of anthropogenic emissions to surface BC were 76% and 80% of total emissions (50% and 59% from gas flaring) for each dataset, respectively.
- The most significant model overestimation was observed in February 2020 when air masses passed through non gas flaring regions. The largest underestimation occurred in April 2020 during the period of spring agriculture fires.
- Daily BB emissions from CAMS were more efficient in representing pollution episodes than monthly GFED4 emissions, and therefore they were used here.
- Russian emissions dominate during the whole year, European and Asian contribute up to 20% in the cold period. Pollution episodes with EBC concentrations above 90 ng/m^3 occur in 18.5% of observation time. Monthly average FLR emissions dominate (98%) any other emission sector.
- FLR and BB emissions contribute the largest share of EBC to the "Island Bely" station during the cold and warm period, respectively. This is consistent with previously-observed source contribution in the Russian Arctic. When air is transported from Europe, other sources such as TRA become important. The same applies for SHP emissions that become important in summertime, because of cruise activities and ice retreat.
- Emissions from the gas and oil fields in Western Siberia, and the Northern European part of Russia cause the vast majority of the pollution episodes in the Arctic.
- 15 pollution episodes with concentrations reaching close to 500 ng/m3 were detected. The duration of the cold pollution episodes is longer than of the warm period, and the median (up to 160 ng/m3) and maximum EBC (up to 450 ng/m3) higher.

In conclusion, the significance of high-quality measurements in the "Island Bely" station is pronounced, because (i) the station is located along the main pathway of airmasses entering the Arctic, and (ii) it is north of the world's largest gas flaring regions. The operation of the "Island Bely" station is an asset in source emission optimisation, because EBC measurements in the High Arctic are still rare.

https://doi.org/10.5194/acp-2021-867
Preprint. Discussion started: 13 December 2021

Atmospheric Chemistry and Physics Discussions

Data availability. All model data used in the present publication together with all figures of footprint analysis and source contributions to surface BC are open through the websites https://niflheim.nilu.no/NikolaosPY/Bely_2020_cams.py and https://niflheim.nilu.no/NikolaosPY/Bely_2020_huang_cams.py. All row model data can be obtained from the corresponding author upon request. The definitions of the regions and continents used in the current analysis are based on regional masks that can be seen in Supplementary Figure S 3.

Competing interests. The authors declare no competing interests.

Acknowledgements. This research was performed in the frame of the Development program of the Interdisciplinary Scientific and Educational School of M. V. Lomonosov Moscow State University "Future Planet and Global Environmental Change". Authors wish to thank much Dr. Tony Hanson (Magee Scientific) for his huge support on the AE33 aethalometer installation and operation at the "Island Bely" station.

Financial support. Development of the methodology for aethalometric measurements and AAE calculations was performed in the frame of RSF project #19 -77-30004. All model and code development and calculations were supported by the COMBAT (Quantification of Global Ammonia Sources constrained by a Bayesian Inversion Technique) project funded by ROMFORSK – Program for romforskning of the Research Council of Norway (Project ID: 275407, website: https://prosjektbanken.forskningsradet.no/project/FORISS/275407?Kilde=FORISS&distribution=Ar&chart=bar&calcType=funding&Sprak=no&sortBy=date&sortOrder=desc&resultCount=30&offset=0&ProgAkt.3=ROMFORSK-Program+for+romforskning) and the EC Horizon 2020 – Research and Innovation Framework Programme ATMO-ACCESS Integrating Activity under grant agreement No 101008004.

Author contributions. O.B.P. supervised the station operation, interpreted data and wrote the manuscript. N.E. performed all the FLEXPART simulations and analyses, wrote and coordinated the paper. V.O.K. analyzed the data. M.A.C. prepared the figures and assisted in the interpretation of the results. K.E. provided BB impact and AAE aging evaluation. A.G. performed AAE calculations and evaluation of data quality. N.S.K. supported the research. All authors contributed to the final version of the manuscript.

https://doi.org/10.5194/acp-2021-867
Preprint. Discussion started: 13 December 2021

Atmospheric Chemistry and Physics Discussions

References

Akagi, S., Yokelson, R. J., Wiedinmyer, C., Alvarado, M., Reid, J., Karl, T., Crounse, J., and Wennberg, P.: Emission factors for open and domestic biomass burning for use in atmospheric models, Atmospheric Chemistry and Physics, 11, 4039-4072, 2011.

Andreae, M. O. and Merlet, P.: Emission of trace gases and aerosols from biomass burning, Global biogeochemical cycles, 15, 955-966, 2001.

Bond, T. C., Doherty, S. J., Fahey, D., Forster, P., Berntsen, T., DeAngelo, B., Flanner, M., Ghan, S., Kärcher, B., and Koch, D.: Bounding the role of black carbon in the climate system: A scientific assessment, Journal of Geophysical Research: Atmospheres, 118, 5380-5552, 2013.

Böttcher, K., Paunu, V.-V., Kupiainen, K., Zhizhin, M., Matveev, A., Savolahti, M., Klimont, Z., Väätäinen, S., Lamberg, H., and Karvosenoja, N.: Black carbon emissions from flaring in Russia in the period 2012-2017, Atmospheric Environment, 118390, 2021.

Cappa, C. D., Kolesar, K. R., Zhang, X., Atkinson, D. B., Pekour, M. S., Zaveri, R. A., Zelenyuk, A., and Zhang, Q.: Understanding the optical properties of ambient sub- and supermicron particulate matter: results from the CARES 2010 field study in northern California, Atmos. Chem. Phys., 16, 6511-6535, 10.5194/acp-16-6511-2016, 2016.

Cassiani, M., Stohl, A., and Brioude, J.: Lagrangian stochastic modelling of dispersion in the convective boundary layer with skewed turbulence conditions and a vertical density gradient: Formulation and implementation in the FLEXPART model, Boundary-Layer Meteorology, 154, 367-390, 2015.

Chang, R.-W., Leck, C., Graus, M., Müller, M., Paatero, J., Burkhart, J. F., Stohl, A., Orr, L., Hayden, K., and Li, S.-M.: Aerosol composition and sources in the central Arctic Ocean during ASCOS, Atmospheric Chemistry and Physics, 2011.

Cho, M.-H., Park, R. J., Yoon, J., Choi, Y., Jeong, J. I., Labzovskii, L., Fu, J. S., Huang, K., Jeong, S.-J., and Kim, B.-M.: A missing component of Arctic warming: black carbon from gas flaring, Environmental Research Letters, 14, 094011, 2019.

Conrad, B. M. and Johnson, M. R.: Field measurements of black carbon yields from gas flaring, Environmental science & technology, 51, 1893-1900, 2017.

Di Giuseppe, F., Remy, S., Pappenberger, F., and Wetterhall, F.: Improving CAMS biomass burning estimations by means of the Global ECMWF Fire Forecast system (GEFF), ECMWF Tech. Memo. 790, 18 pp., https://www. ecmwf. int/sites/default/files …, 2016.

Drinovec, L., Močnik, G., Zotter, P., Prévôt, A., Ruckstuhl, C., Coz, E., Rupakheti, M., Sciare, J., Müller, T., and Wiedensohler, A.: The" dual-spot" Aethalometer: an improved measurement of aerosol black carbon with real-time loading compensation, Atmospheric Measurement Techniques, 8, 1965-1979, 2015.

Eckhardt, S., Quennehen, B., Olivié, D. J. L., Berntsen, T. K., Cherian, R., Christensen, J. H., Collins, W., Crepinsek, S., Daskalakis, N., Flanner, M., Herber, A., Heyes, C., Hodnebrog, Ø., Huang, L., Kanakidou, M., Klimont, Z., Langner, J., Law, K. S., Lund, M. T., Mahmood, R., Massling, A., Myriokefalitakis, S., Nielsen, I. E., Nøjgaard, J. K., Quaas, J., Quinn, P. K., Raut, J. C., Rumbold, S. T., Schulz, M., Sharma, S., Skeie, R. B., Skov, H., Uttal, T., von Salzen, K., and Stohl, A.: Current model capabilities for simulating black carbon and sulfate concentrations in the Arctic atmosphere: a multi-model evaluation using a comprehensive measurement data set, Atmos. Chem. Phys., 15, 9413-9433, 10.5194/acp-15-9413-2015, 2015.

Eleftheriadis, K., Vratolis, S., and Nyeki, S.: Aerosol black carbon in the European Arctic: Measurements at Zeppelin station, Ny-Ålesund, Svalbard from 1998–2007, Geophysical Research Letters, 36, n/a-n/a, 10.1029/2008GL035741, 2009.

Eleftheriadis, K., Nyeki, S., Psomiadou, C., and Colbeck, I.: Background aerosol properties in the European arctic, Water, Air and Soil Pollution: Focus, 4, 23-30, 2004.

Flanner, M. G.: Arctic climate sensitivity to local black carbon, Journal of Geophysical Research: Atmospheres, 118, 1840-1851, 10.1002/jgrd.50176, 2013.

https://doi.org/10.5194/acp-2021-867
Preprint. Discussion started: 13 December 2021

Atmospheric Chemistry and Physics Discussions

660 Forrister, H., Liu, J., Scheuer, E., Dibb, J., Ziemba, L., Thornhill, K. L., Anderson, B., Diskin,
661 G., Perring, A. E., and Schwarz, J. P.: Evolution of brown carbon in wildfire plumes,
662 Geophysical Research Letters, 42, 4623-4630, 2015.
663 Forster, C., Stohl, A., and Seibert, P.: Parameterization of convective transport in a Lagrangian
664 particle dispersion model and its evaluation, Journal of applied meteorology and climatology, 46,
665 403-422, 2007.
666 Giglio, L., Randerson, J. T., and Van Der Werf, G. R.: Analysis of daily, monthly, and annual
667 burned area using the fourth-generation global fire emissions database (GFED4), Journal of
668 Geophysical Research: Biogeosciences, 118, 317-328, 2013.
669 Grange, S. K., Lötscher, H., Fischer, A., Emmenegger, L., and Hueglin, C.: Evaluation of
670 equivalent black carbon source apportionment using observations from Switzerland between
671 2008 and 2018, Atmospheric Measurement Techniques, 13, 1867-1885, 2020.
672 Grythe, H., Kristiansen, N. I., Groot Zwaaftink, C. D., Eckhardt, S., Ström, J., Tunved, P.,
673 Krejci, R., and Stohl, A.: A new aerosol wet removal scheme for the Lagrangian particle model
674 FLEXPART v10, Geosci. Model Dev., 10, 1447-1466, 10.5194/gmd-10-1447-2017, 2017.
675 Helin, A., Virkkula, A., Backman, J., Pirjola, L., Sippula, O., Aakko-Saksa, P., Väätäinen, S.,
676 Mylläri, F., Järvinen, A., and Bloss, M.: Variation of absorption Ångström exponent in aerosols
677 from different emission sources, Journal of Geophysical Research: Atmospheres, 126,
678 e2020JD034094, 2021.
679 Huang, K., Fu, J. S., Prikhodko, V. Y., Storey, J. M., Romanov, A., Hodson, E. L., Cresko, J.,
680 Morozova, I., Ignatieva, Y., and Cabaniss, J.: Russian anthropogenic black carbon: Emission
681 reconstruction and Arctic black carbon simulation, Journal of Geophysical Research:
682 Atmospheres, 120, 11,306-311,333, 2015.
683 Ismail, O. S. and Umukoro, G. E.: Global impact of gas flaring, Energy and Power Engineering,
684 4, 290, 2012.
685 Johnson, M. S., Strawbridge, K., Knowland, K. E., Keller, C., and Travis, M.: Long-range
686 transport of Siberian biomass burning emissions to North America during FIREX-AQ,
687 Atmospheric Environment, 252, 118241, 2021.
688 Kaiser, J., Heil, A., Andreae, M., Benedetti, A., Chubarova, N., Jones, L., Morcrette, J.-J.,
689 Razinger, M., Schultz, M., and Suttie, M.: Biomass burning emissions estimated with a global
690 fire assimilation system based on observed fire radiative power, Biogeosciences, 9, 527-554,
691 2012.
692 Kalogridis, A.-C., Vratolis, S., Liakakou, E., Gerasopoulos, E., Mihalopoulos, N., and
693 Eleftheriadis, K.: Assessment of wood burning versus fossil fuel contribution to wintertime black
694 carbon and carbon monoxide concentrations in Athens, Greece, Atmospheric Chemistry and
695 Physics, 18, 10219-10236, 2018a.
696 Kalogridis, A. C., Popovicheva, O. B., Engling, G., Diapouli, E., Kawamura, K., Tachibana, E.,
697 Ono, K., Kozlov, V. S., and Eleftheriadis, K.: Smoke aerosol chemistry and aging of Siberian
698 biomass burning emissions in a large aerosol chamber, Atmospheric Environment, 185, 15-28,
699 https://doi.org/10.1016/j.atmosenv.2018.04.033, 2018b.
700 Kaufman, Y., Ichoku, C., Giglio, L., Korontzi, S., Chu, D., Hao, W., Li, R.-R., and Justice, C.:
701 Fire and smoke observed from the Earth Observing System MODIS instrument--products,
702 validation, and operational use, International Journal of Remote Sensing, 24, 1765-1781, 2003.
703 Klimont, Z., Kupiainen, K., Heyes, C., Purohit, P., Cofala, J., Rafaj, P., Borken-Kleefeld, J., and
704 Schöpp, W.: Global anthropogenic emissions of particulate matter including black carbon,
705 Atmospheric Chemistry and Physics Discussions, 17, 8681-8723, 2017.
706 Kozlov, V. S., Panchenko, M. V., Shmargunov, V. P., Chernov, D. G., Yausheva, E. P., Pol'kin,
707 V. V., and Terpugova, S. A.: Long-term investigations of the spatiotemporal variability of black
708 carbon and aerosol concentrations in the troposphere of West Siberia and Russian Subarctic,
709 Химия в интересах устойчивого развития, 24, 423-440, 2016.

https://doi.org/10.5194/acp-2021-867
Preprint. Discussion started: 13 December 2021

Long, C. M., Nascarella, M. A., and Valberg, P. A.: Carbon black vs. black carbon and other airborne materials containing elemental carbon: Physical and chemical distinctions, Environmental Pollution, 181, 271-286, 2013.
Manousakas, M., Popovicheva, O., Evangeliou, N., Diapouli, E., Sitnikov, N., Shonija, N., and Eleftheriadis, K.: Aerosol carbonaceous, elemental and ionic composition variability and origin at the Siberian High Arctic, Cape Baranova, Tellus B: Chemical and Physical Meteorology, 72, 1-14, 2020.
Paris, J.-D., Stohl, A., Nédélec, P., Arshinov, M. Y., Panchenko, M., Shmargunov, V., Law, K. S., Belan, B., and Ciais, P.: Wildfire smoke in the Siberian Arctic in summer: source characterization and plume evolution from airborne measurements, Atmospheric Chemistry and Physics, 9, 9315-9327, 2009.
Pisso, I., Sollum, E., Grythe, H., Kristiansen, N. I., Cassiani, M., Eckhardt, S., Arnold, D., Morton, D., Thompson, R. L., and Groot Zwaaftink, C. D.: The Lagrangian particle dispersion model FLEXPART version 10.4, Geoscientific Model Development, 12, 4955-4997, 2019.
Popovicheva, O., Chichaeva, M., Kobelev, V., Sinitskiy, A., and Hansen, A.: Black Carbon in urban emissions on the Polar Circle, 26th International Symposium on Atmos. Ocean Optics, Proc. SPIE, 11560J,
Popovicheva, O., Timofeev, M., Persiantseva, N., Jefferson, M. A., Johnson, M., Rogak, S. N., and Baldelli, A.: Microstructure and chemical composition of particles from small-scale gas flaring, Aerosol and Air Quality Research, 19, 2205-2221, 2019a.
Popovicheva, O., Diapouli, E., Makshtas, A., Shonija, N., Manousakas, M., Saraga, D., Uttal, T., and Eleftheriadis, K.: East Siberian Arctic background and black carbon polluted aerosols at HMO Tiksi, Science of the Total Environment, 655, 924-938, 2019b.
Popovicheva, O. B., Evangeliou, N., Eleftheriadis, K., Kalogridis, A. C., Sitnikov, N., Eckhardt, S., and Stohl, A.: Black Carbon Sources Constrained by Observations in the Russian High Arctic, Environmental Science & Technology, 51, 3871-3879, 10.1021/acs.est.6b05832, 2017.
Qi, L. and Wang, S.: Sources of black carbon in the atmosphere and in snow in the Arctic, Science of The Total Environment, 691, 442-454, 2019.
Quinn, P. K., Bates, T. S., Baum, E., Doubleday, N., Fiore, A. M., Flanner, M., Fridlind, A., Garrett, T. J., Koch, D., Menon, S., Shindell, D., Stohl, A., and Warren, S. G.: Short-lived pollutants in the Arctic: their climate impact and possible mitigation strategies, Atmos. Chem. Phys., 8, 1723-1735, 10.5194/acp-8-1723-2008, 2008.
Randerson, J., Chen, Y., Van Der Werf, G., Rogers, B., and Morton, D.: Global burned area and biomass burning emissions from small fires, Journal of Geophysical Research: Biogeosciences, 117, 2012.
Ren, L., Yang, Y., Wang, H., Zhang, R., Wang, P., and Liao, H.: Source attribution of Arctic black carbon and sulfate aerosols and associated Arctic surface warming during 1980–2018, Atmospheric Chemistry and Physics, 20, 9067-9085, 2020.
Romshoo, B., Müller, T., Pfeifer, S., Saturno, J., Nowak, A., Ciupek, K., Quincey, P., and Wiedensohler, A.: Optical properties of coated black carbon aggregates: numerical simulations, radiative forcing estimates, and size-resolved parameterization scheme, Atmos. Chem. Phys., 21, 12989-13010, 10.5194/acp-21-12989-2021, 2021.
Saleh, R., Hennigan, C., McMeeking, G., Chuang, W., Robinson, E., Coe, H., Donahue, N., and Robinson, A.: Absorptivity of brown carbon in fresh and photo-chemically aged biomass-burning emissions, Atmospheric Chemistry and Physics, 13, 7683-7693, 2013.
Sandradewi, J., Prévôt, A. S., Szidat, S., Perron, N., Alfarra, M. R., Lanz, V. A., Weingartner, E., and Baltensperger, U.: Using aerosol light absorption measurements for the quantitative determination of wood burning and traffic emission contributions to particulate matter, Environmental science & technology, 42, 3316-3323, 2008.
Schacht, J., Heinold, B., Quaas, J., Backman, J., Cherian, R., Ehrlich, A., Herber, A., Huang, W. T. K., Kondo, Y., Massling, A., Sinha, P. R., Weinzierl, B., Zanatta, M., and Tegen, I.: The importance of the representation of air pollution emissions for the modeled distribution and

https://doi.org/10.5194/acp-2021-867
Preprint. Discussion started: 13 December 2021

Atmospheric Chemistry and Physics Discussions

762 radiative effects of black carbon in the Arctic, Atmos. Chem. Phys., 19, 11159-11183,
763 10.5194/acp-19-11159-2019, 2019.
764 Sharma, S., Lavoué, D., Cachier, H., Barrie, L., and Gong, S.: Long-term trends of the black
765 carbon concentrations in the Canadian Arctic, Journal of Geophysical Research: Atmospheres,
766 109, 2004.
767 Stathopoulos, V., Evangeliou, N., Stohl, A., Vratolis, S., Matsoukas, C., and Eleftheriadis, K.:
768 Large circulation patterns strongly modulate long term variability of Arctic black carbon levels
769 and areas of origin, Geophysical Research Letters, e2021GL092876, 2021.
770 Stohl, A.: Characteristics of atmospheric transport into the Arctic troposphere, Journal of
771 Geophysical Research: Atmospheres, 111, n/a-n/a, 10.1029/2005JD006888, 2006.
772 Stohl, A., Forster, C., Frank, A., Seibert, P., and Wotawa, G.: Technical note: The Lagrangian
773 particle dispersion model FLEXPART version 6.2, Atmos. Chem. Phys., 5, 2461-2474,
774 10.5194/acp-5-2461-2005, 2005.
775 Stohl, A., Klimont, Z., Eckhardt, S., Kupiainen, K., Shevchenko, V. P., Kopeikin, V. M., and
776 Novigatsky, A. N.: Black carbon in the Arctic: the underestimated role of gas flaring and
777 residential combustion emissions, Atmos. Chem. Phys., 13, 8833-8855, 10.5194/acp-13-8833-
778 2013, 2013.
779 Stohl, A., Andrews, E., Burkhart, J., Forster, C., Herber, A., Hoch, S., Kowal, D., Lunder, C.,
780 Mefford, T., and Ogren, J.: Pan-Arctic enhancements of light absorbing aerosol concentrations
781 due to North American boreal forest fires during summer 2004, Journal of Geophysical
782 Research: Atmospheres, 111, 2006.
783 Stohl, A., Berg, T., Burkhart, J., Fjæraa, A., Forster, C., Herber, A., Hov, Ø., Lunder, C.,
784 McMillan, W., and Oltmans, S.: Arctic smoke–record high air pollution levels in the European
785 Arctic due to agricultural fires in Eastern Europe in spring 2006, Atmospheric Chemistry and
786 Physics, 7, 511-534, 2007.
787 Stone, R. S., Sharma, S., Herber, A., Eleftheriadis, K., and Nelson, D. W.: A characterization of
788 Arctic aerosols on the basis of aerosol optical depth and black carbon measurements, Elem Sci
789 Anth, 2, 2014.
790 Treffeisen, R., Turnved, P., StrÖm, J., Herber, A., Bareiss, J., Helbig, A., Stone, R. S.,
791 Hoyningen-Huene, W., Krejci, R., Stohl, A., and Neuber, R.: Arctic smoke ? aerosol
792 characteristics during a record air pollution event in the European Arctic and its radiative impact,
793 Atmospheric Chemistry and Physics Discussions, 7, 2275-2324, 2007.
794 Tunved, P., Ström, J., and Krejci, R.: Arctic aerosol life cycle: linking aerosol size distributions
795 observed between 2000 and 2010 with air mass transport and precipitation at Zeppelin station,
796 Ny-Å lesund, Svalbard, Atmospheric Chemistry & Physics, 13, 3643-3660, 2013.
797 Vinogradova, A.: Anthropogenic Black Carbon emissions to the atmosphere: surface distribution
798 through Russian territory, Atmospheric and Oceanic Optics, 28, 158-164, 2015.
799 Virkkula, A.: Modeled source apportionment of black carbon particles coated with a light-
800 scattering shell, Atmospheric Measurement Techniques, 14, 3707-3719, 2021.
801 Voronova, O., Zima, A., Kladov, V., and Cherepanova, E.: Anomalous Wildfires in Siberia in
802 Summer 2019, Izvestiya, Atmospheric and Oceanic Physics, 56, 1042-1052, 2020.
803 Wang, Q., Jacob, D. J., Fisher, J. A., Mao, J., Leibensperger, E. M., Carouge, C. C., Le Sager, P.,
804 Kondo, Y., Jimenez, J. L., Cubison, M. J., and Doherty, S. J.: Sources of carbonaceous aerosols
805 and deposited black carbon in the Arctic in winter-spring: implications for radiative forcing,
806 Atmos. Chem. Phys., 11, 12453-12473, 10.5194/acp-11-12453-2011, 2011.
807 Warneke, C., Froyd, K., Brioude, J., Bahreini, R., Brock, C., Cozic, J., De Gouw, J., Fahey, D.,
808 Ferrare, R., and Holloway, J.: An important contribution to springtime Arctic aerosol from
809 biomass burning in Russia, Geophysical Research Letters, 37, 2010.
810 Werf, G. R., Randerson, J. T., Giglio, L., Leeuwen, T. T. v., Chen, Y., Rogers, B. M., Mu, M.,
811 Van Marle, M. J., Morton, D. C., and Collatz, G. J.: Global fire emissions estimates during
812 1997–2016, Earth System Science Data, 9, 697-720, 2017.

https://doi.org/10.5194/acp-2021-867
Preprint. Discussion started: 13 December 2021

Winiger, P., Andersson, A., Eckhardt, S., Stohl, A., and Gustafsson, Ö.: The sources of atmospheric black carbon at a European gateway to the Arctic, Nature communications, 7, 1-8, 2016.

Winiger, P., Andersson, A., Eckhardt, S., Stohl, A., Semiletov, I. P., Dudarev, O. V., Charkin, A., Shakhova, N., Klimont, Z., Heyes, C., and Gustafsson, Ö.: Siberian Arctic black carbon sources constrained by model and observation, Proceedings of the National Academy of Sciences, 114, E1054-E1061, 10.1073/pnas.1613401114, 2017.

Wooster, M. J., Roberts, G., Perry, G., and Kaufman, Y.: Retrieval of biomass combustion rates and totals from fire radiative power observations: FRP derivation and calibration relationships between biomass consumption and fire radiative energy release, Journal of Geophysical Research: Atmospheres, 110, 2005.

Yun, Y., Penner, J. E., and Popovicheva, O.: The effects of hygroscopicity on ice nucleation of fossil fuel combustion aerosols in mixed-phase clouds, Atmos. Chem. Phys., 13, 4339-4348, 10.5194/acp-13-4339-2013, 2013.

Zhu, C., Kanaya, Y., Takigawa, M., Ikeda, K., Tanimoto, H., Taketani, F., Miyakawa, T., Kobayashi, H., and Pisso, I.: FLEXPART v10. 1 simulation of source contributions to Arctic black carbon, Atmospheric Chemistry and Physics, 20, 1641-1656, 2020.

Zotter, P., Herich, H., Gysel, M., El-Haddad, I., Zhang, Y., Močnik, G., Hüglin, C., Baltensperger, U., Szidat, S., and Prévôt, A. S.: Evaluation of the absorption Ångström exponents for traffic and wood burning in the Aethalometer-based source apportionment using radiocarbon measurements of ambient aerosol, Atmospheric Chemistry and Physics, 17, 4229-4249, 2017.

https://doi.org/10.5194/acp-2021-867
Preprint. Discussion started: 13 December 2021

Atmospheric Chemistry and Physics Discussions

837 **FIGURE LEGENDS**

838

839

840 **Figure 1**. Top left map shows the newly established "Island Bely" aerosol station in contrast to
841 other Arctic stations (Zeppelin, Alert, Barrow, Summit, Tiksi, and Cape Baranova). Bottom left
842 map shows the location of the Bely Island in the Kara Sea, where the new station was developed
843 (73°20'7.57"N, 70°4'49.05"E). The map on the right shows the "Island Bely" aerosol station in
844 combination with the European part of Russia and Western Siberia and the Yamalo-Nenets
845 Autonomic Okrug (YNAO). Flares of oil and gas fields are shown for 2019 year in brown triangles
846 (adopted from https://skytruth.org/).

847

https://doi.org/10.5194/acp-2021-867
Preprint. Discussion started: 13 December 2021

Atmospheric Chemistry and Physics Discussions

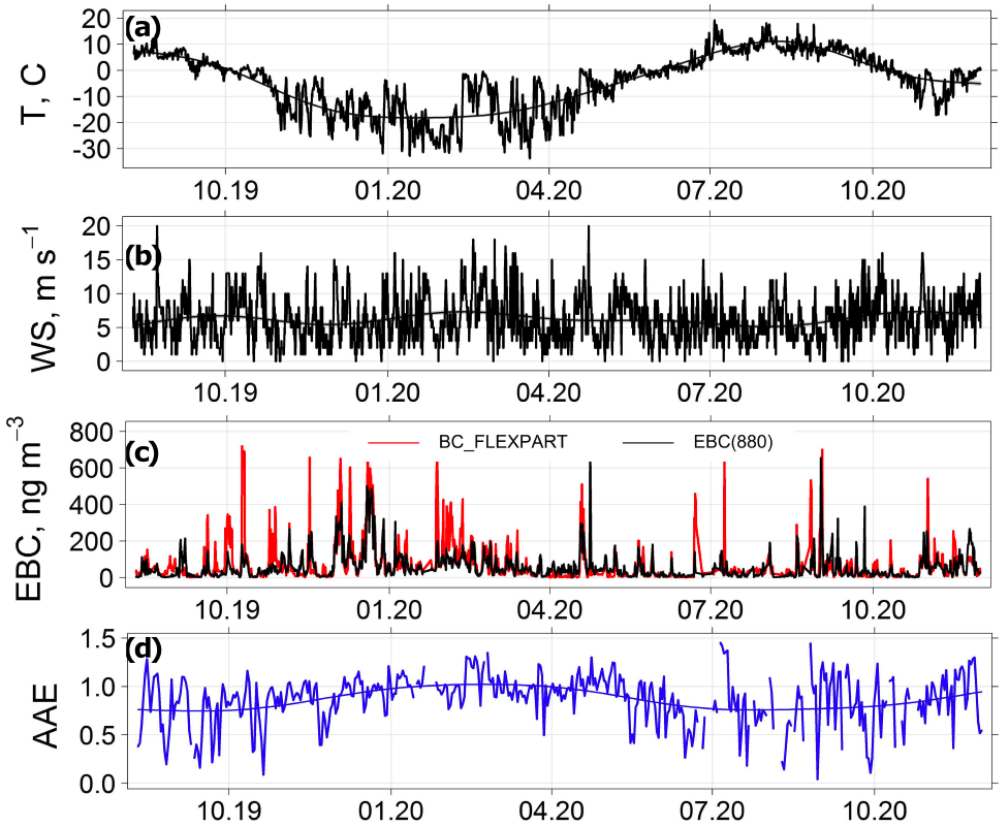

Figure 2. Meteorological conditions with respect to (a) mean temperature and (b) wind speed (data were smoothed to show long-term variations), time-series of (c) 24h median EBC (black) and model simulated BC using ECLIPSEv6 - CAMS emissions (red), and (d) 24h average absorption Ångström exponent (AAE) measured at "Island Bely" station from 10 August 2019 to 30 November 2020 (date format in mm.yy).

https://doi.org/10.5194/acp-2021-867
Preprint. Discussion started: 13 December 2021

Atmospheric Chemistry and Physics Discussions

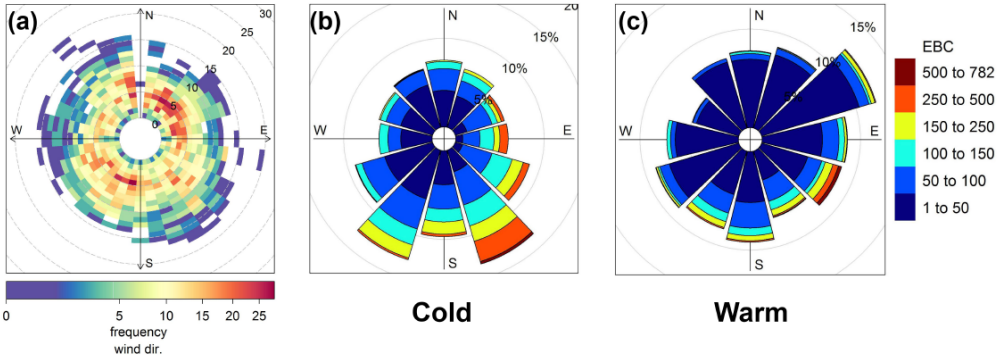

855

856 **Figure 3**. (a) Polar frequency plot of wind speed and direction. Each cell gives the total number
857 of hours the wind was originating from a certain wind direction. The dashed circular grey lines
858 show the wind speed (in m s^{-1}). Rose diagrams showing 3h EBC concentrations during the cold
859 (b) and warm (c) periods.

860

https://doi.org/10.5194/acp-2021-867
Preprint. Discussion started: 13 December 2021

Atmospheric Chemistry and Physics Discussions

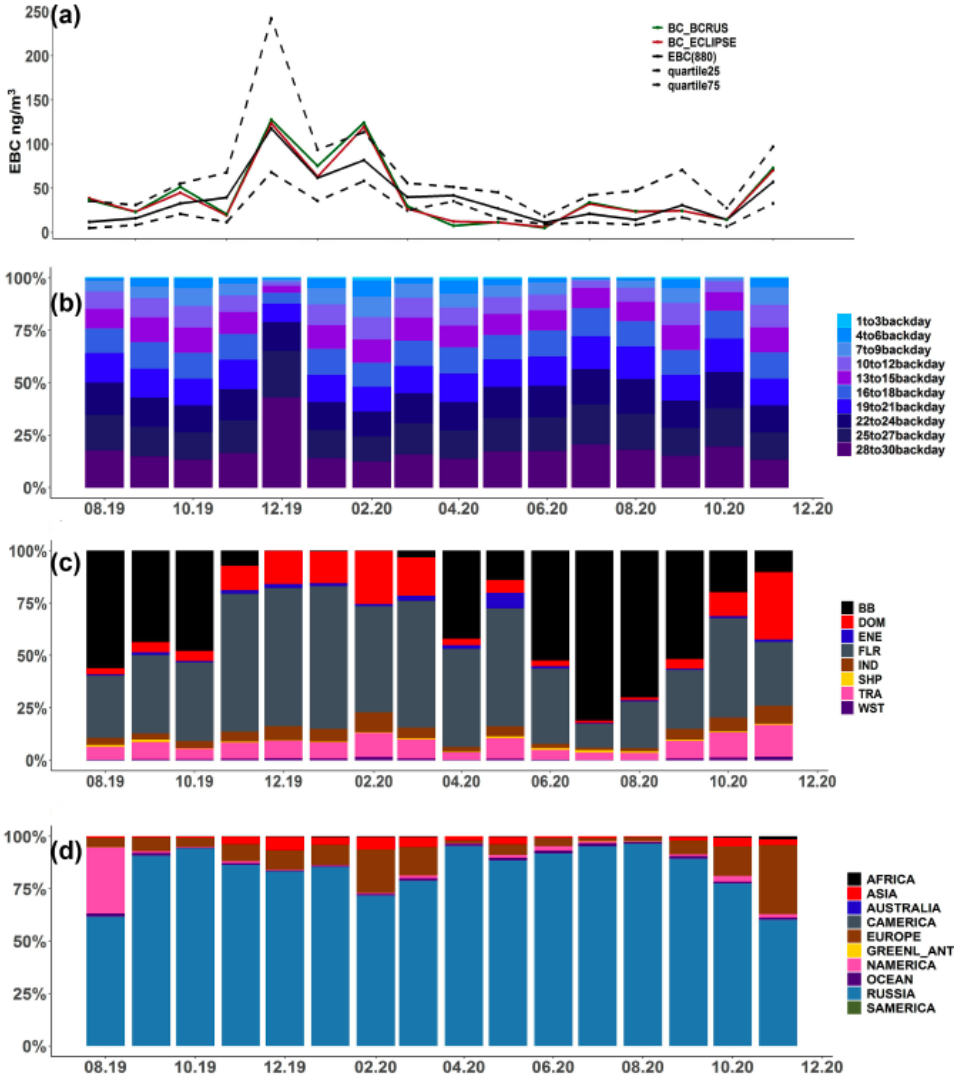

Figure 4. (a) Monthly climatology of EBC at the "Island Bely" station depicting medians, 25th and 75th percentiles (dashed lines). Near-surface monthly median BC mass concentrations simulated with FLEXPART with ECLIPSEv6-CAMS (steel blue) and ECLIPSEv6-BCRUS-CAMS (red) emissions are also shown. (b) Age spectrum of modelled BC from all possible sources showing the contribution of emissions each day back in time to the surface concentration of BC. (c) Contribution from different emission source types to surface BC concentrations. The emission sources of biomass burning (BB) adopted from GFEDv4.1, and residential and commercial (DOM), power plants, energy conversion, and extraction (ENE), gas flaring (FLR), industrial combustion and processing (IND), shipping (SHP), nd transportation (TRA) adopted from ECLIPSEv6 inventories were considered. (d) Continental spectrum showing the contribution of each continent or region to surface concentrations of BC. 10 regions were considered namely, Africa, Asia, Australia, Central America, Europe, Greenland/Antarctica, North America, World Ocean, Russia, and South America (see Supplementary Figure S 3).

https://doi.org/10.5194/acp-2021-867
Preprint. Discussion started: 13 December 2021

Atmospheric Chemistry and Physics Discussions

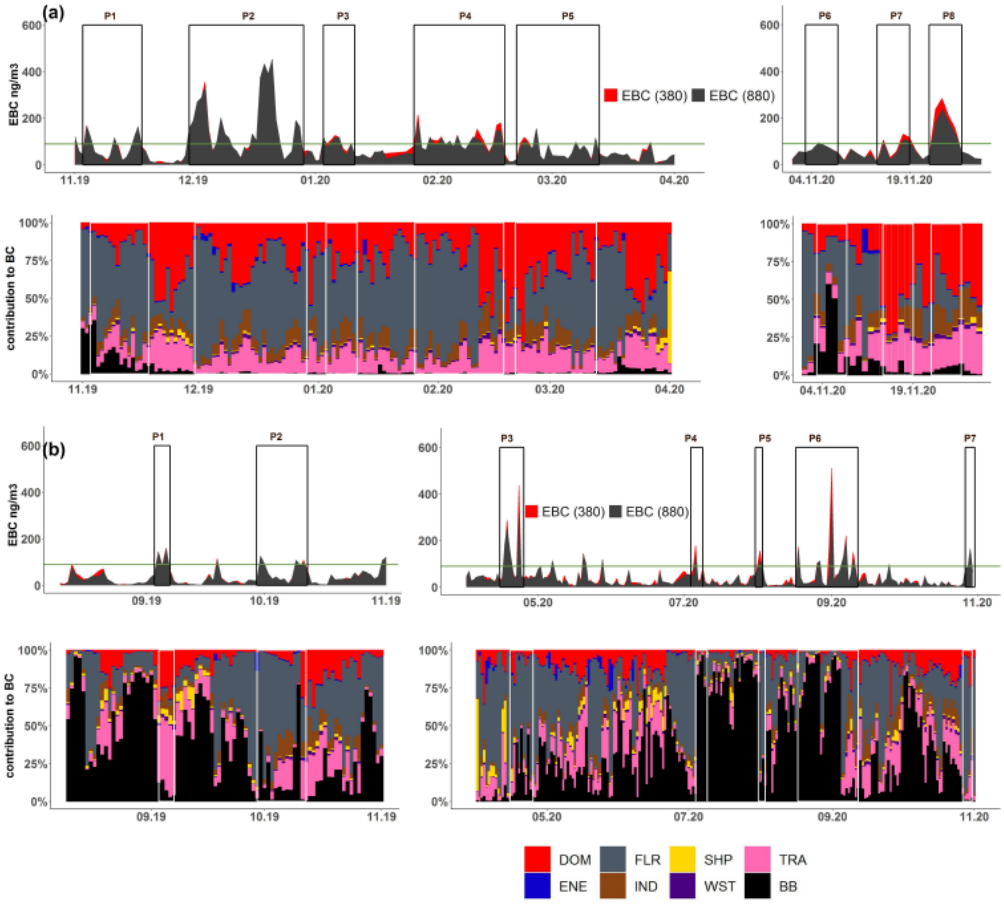

875

876 **Figure 5**. 24-hour median EBC concentrations measured at 880 nm (black) and 370 nm (red), and
877 source contributions to surface BC from anthropogenic (DOM, ENE, FLR, IND, SHP, WST,
878 TRA) and BB sources for (a) the cold and (b) the warm period. Pollution episodes (P1-P8) are
879 composed from the periodically repeated events of highest EBC concentration. The green straight
880 line indicates the pollution level of the 80th percentile.

881

https://doi.org/10.5194/acp-2021-867
Preprint. Discussion started: 13 December 2021

Atmospheric Chemistry and Physics Discussions

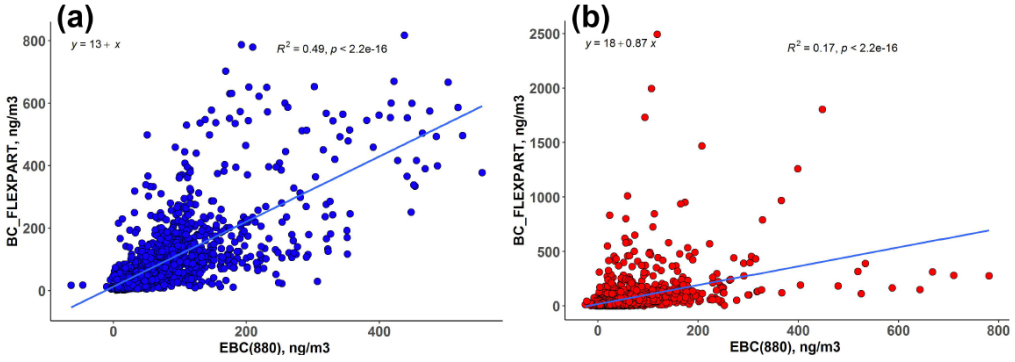

882

883 **Figure 6**. Scatter-plots of 3h median measured EBC (880) and modelled BC from FLEXPART
884 for the (a) cold and (b) warm period. Solid line is the linear regression fit of the comparison
885 between modelled and observed values.

886

https://doi.org/10.5194/acp-2021-867
Preprint. Discussion started: 13 December 2021

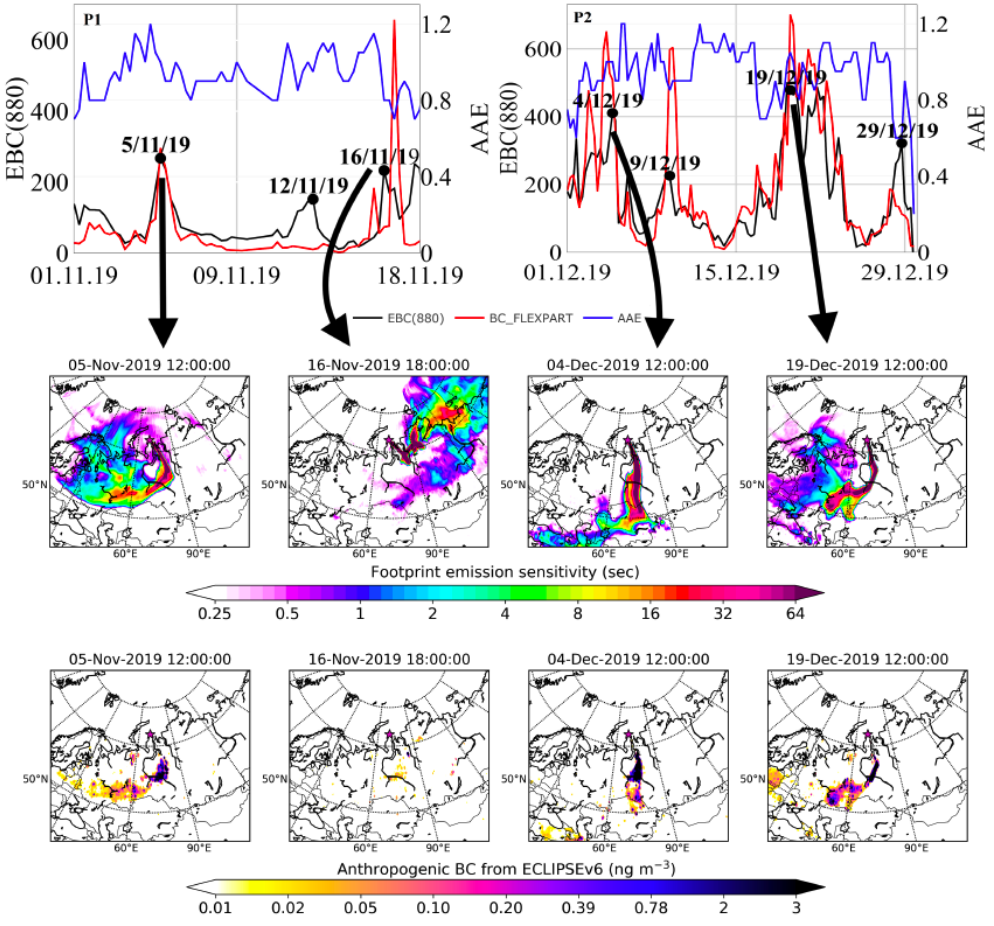

Figure 7. Examples of pollution episodes P1 and P2 observed in the cold period (see **Figure 5**a), where FLR contribution prevails. 6-hourly median EBC (880) (black line), BC simulated with FLEXPART (red line), AAE (blue line) (upper row). Footprint emissions sensitivities in seconds showing the largest probability of emission origin (middle row). Spatial distribution of anthropogenic contribution (in ng/m3) to surface BC at the "Island Bely" station.

https://doi.org/10.5194/acp-2021-867
Preprint. Discussion started: 13 December 2021

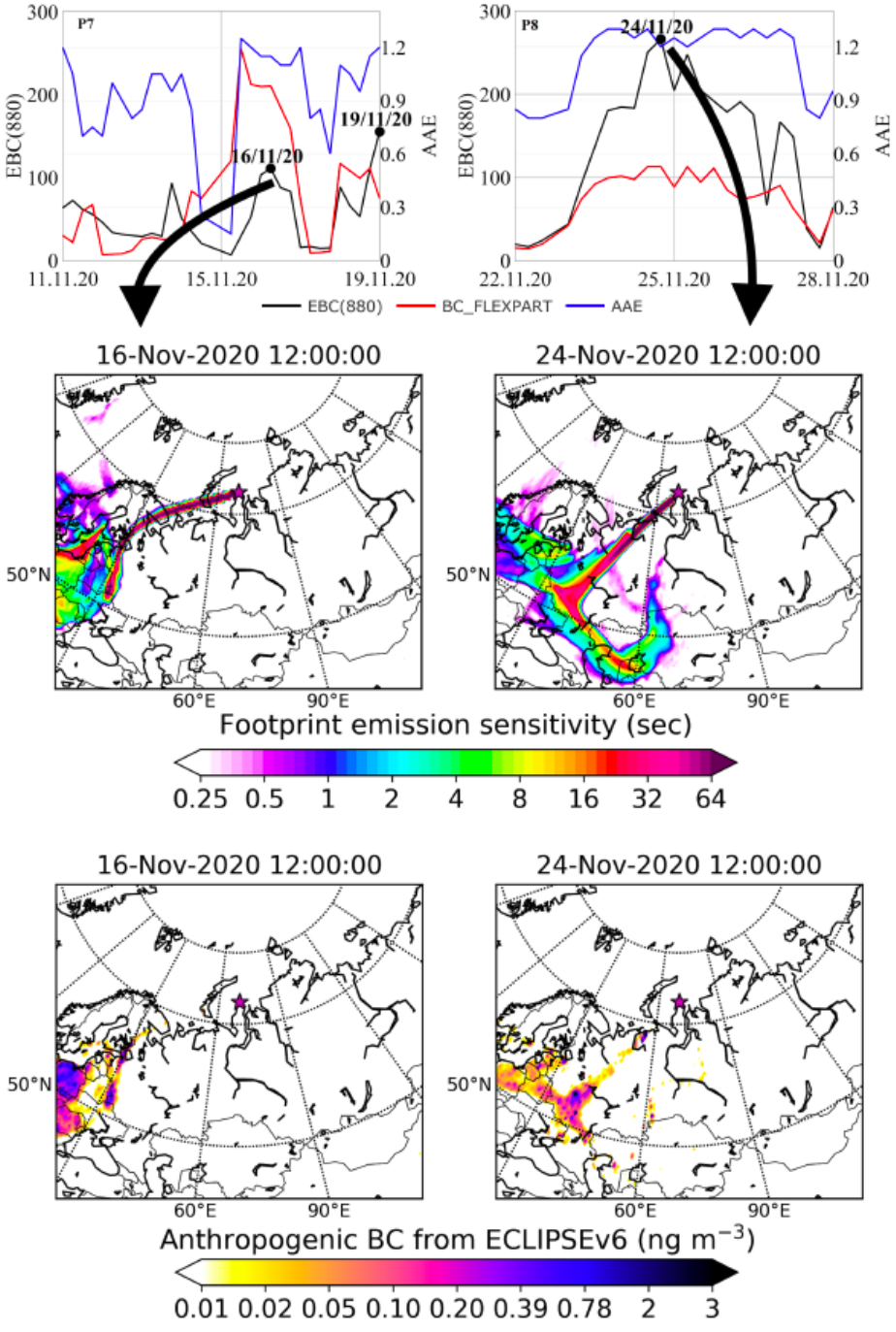

Figure 8. Examples of pollution episodes P7 and P8 observed in the cold period (see **Figure 5**a), where DOM and TRA contribution prevails. Timeseries of measured EBC, modelled BC and AAE, footprint emissions sensitivities and anthropogenic contribution to surface BC are shown.

https://doi.org/10.5194/acp-2021-867
Preprint. Discussion started: 13 December 2021

Atmospheric Chemistry and Physics Discussions

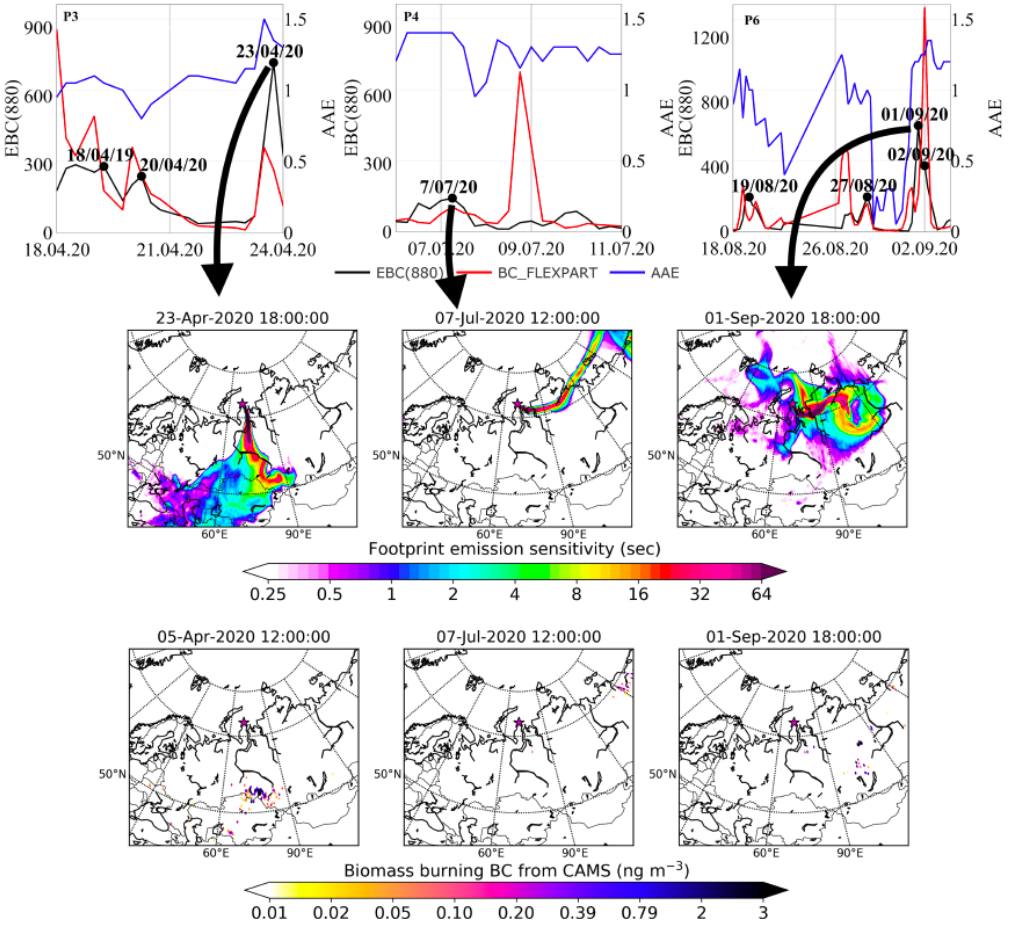

Figure 9. Examples of pollution episodes P3, P4 and P6 in the warm period (see **Figure 5**b), where BB contribution prevails. The figure has been arranged similar to **Figure 7** (timeseries of measured EBC, modelled BC and AAE, footprint emissions sensitivities and BB contribution to surface BC).